EGTRIB Journal
JOURNAL OF
THE EGYPTIAN SOCIETY OF TRIBOLOGY
VOLUME 22, No. 3, July 2025, pp. 98 - 113 **ISSN 2090 - 5882**
(Received May 13. 2025, Accepted in final form June 24. 2025) **jest.journals.ekb.eg**

TRIBOLOGICAL AND ELECTROCHEMICAL BEHAVIOR OF GRAPHENE, CNT, AND BN REINFORCED AA5083 ALUMINUM MATRIX COMPOSITES

Hussein H.[1] and Moustafa E. B.[2]

[1]Mechanical and Mechatronics Engineering Department, Higher Technological Institute, Tenth of Ramadan City 44637,
[2]Benha National University, EGYPT.

ABSTRACT
This study investigates the influence of nano-scale reinforcements carbon nanotubes (CNTs), hexagonal boron nitride (h-BN), and graphene on the mechanical, tribological, and corrosion-resistant properties of AA5083 aluminum alloy composites. Single- and hybrid-reinforced composites were fabricated using Friction Stir Processing (FSP), and their performance was evaluated through microstructural analysis, microhardness testing, wear rate assessment, and electrochemical corrosion studies. Microstructural characterization revealed a uniform dispersion of reinforcements, particularly in hybrid combinations, resulting in significant grain refinement and enhanced mechanical properties. Among single-reinforced composites, graphene demonstrated the lowest wear rate (0.14 mm³/m) and corrosion rate (0.0127 mm/y), while BN showed the highest hardness improvement (78 HV). Hybrid composites exhibited superior performance due to synergistic effects between reinforcements. The AA5083/BN–G composite achieved the highest hardness (86 HV) and a 61% reduction in wear rate compared to the base alloy. Electrochemical analysis revealed that CNT and graphene significantly enhanced corrosion resistance, with CNT-reinforced composites exhibiting exceptional charge transfer resistance.

KEYWORDS
Nano-reinforced composites, AA5083 aluminum alloy, wear resistance, corrosion behavior, hybrid metal matrix composites.

INTRODUCTION
The addition of single reinforcement particles, particularly silicon carbide (SiC), significantly enhances the mechanical properties of aluminum metal matrix composites (AMMCs). Multiple studies have shown that increasing the weight percentage of SiC particles leads to improved hardness, tensile strength, and wear resistance of AMMCs, [1 - 3]. The hardness of AMMCs can increase by up to 25% compared to pure aluminum alloy, [4]. The distribution of reinforcement particles in the matrix is crucial for achieving optimal properties, [5]. However, higher

percentages of reinforcement particles may reduce the forgeability of the composites. These improved properties make AMMCs suitable for various applications in automotive, aerospace, and electronic industries, [4, 6]. Researchers have investigated various combinations of ceramic particles, industrial waste, and nanoparticles as reinforcements in aluminum matrix composites, [7]. These hybrid composites have shown improvements in hardness, tensile strength, and wear resistance compared to unreinforced alloys, [8, 9]. The addition of nanoparticles has been found to enhance mechanical properties further, with studies reporting increased hardness, tensile strength, and compressive strength as the percentage of reinforcements increases, [10]. Fabrication methods such as stir casting and friction stir processing have been employed to produce these composites, [11]. The improved properties of hybrid aluminum matrix composites make them suitable for applications in aerospace, automotive, and other industries requiring high-performance materials, [12]. Aluminum matrix composites (AMCs) reinforced with single or multiple particles exhibit improved mechanical and tribological properties compared to pure aluminum alloys, [13,14] Common reinforcements include Al_2O_3, SiC, B4C, and graphite, [15, 16] Hybrid AMCs generally demonstrate superior wear resistance and mechanical properties than single-reinforced composites, [13, 17]. Fabrication methods like stir casting and powder metallurgy influence particle distribution and composite properties, [18]. Wear behavior is affected by factors such as reinforcement type, load, speed, and sliding distance (Basavarajappa & Chandramohan, 2005). The addition of graphite particles can form a protective layer on the wear surface, enhancing wear resistance. Increasing reinforcement content generally improves wear resistance and mechanical properties [19]. The addition of reinforcements such as SiC, Al2O3, B4C, and RHA generally improves corrosion resistance, [20, 21]. Single-particle reinforcements, particularly zircon sand, have shown better corrosion resistance compared to dual-particle reinforcements, [22]. The corrosion rate typically decreases with increasing reinforcement content. Hybrid composites, such as Al7075 reinforced with SiC and Al_2O_3, exhibit lower corrosion rates compared to monolithic alloys, [23]. Novel reinforcements, such as MWCNT, have also demonstrated improved corrosion resistance in AA5083 alloy, [25]. These improvements in corrosion behavior, along with enhanced mechanical properties, make aluminum matrix composites a viable option for various industrial applications, [24]. The primary objective of this study is to investigate and improve the mechanical, tribological (wear), and corrosion-resistant properties of AA5083 aluminum alloy through the incorporation of single and hybrid nano-scale reinforcements, namely carbon nanotubes (CNTs), hexagonal boron nitride (h-BN), and graphene. The work aims to evaluate the influence of these reinforcements on microstructure evolution, hardness, wear performance, and electrochemical behavior when integrated into the aluminum matrix using Friction Stir Processing (FSP).

EXPERIMENTAL

Material Preparation and fabrication process

The base material used in this study was AA5083 aluminum alloy. It was machined into rectangular plates of 150 mm × 150 mm × 10 mm. Each was drilled with four rows of cylindrical apertures having uniform diameter and 3 mm depth. Twenty two

grooves were fabricated per plate, resulting in 15 % volume fraction for individual nano-reinforcements (CNT, BN, and G), while hybrid combinations (BN + CNT, BN + G, and CNT + G) incorporated each constituent at 7.5% to maintain the same total reinforcement content. Variations in aperture spacing across rows resulted in differing cavity volumes prior to particle filling. The initial stage of the Friction Stir Processing (FSP) procedure, as shown in Fig. 1, involved precisely filling the pre-machined holes and grooves with selected nano-scale reinforcements to ensure complete and uniform cavity saturation, thereby facilitating effective integration during FSP. Each plate was loaded with a specific combination of nano-additives—namely BN–CNT, BN–G, and BN–G–CNT—arranged in predefined ratios to promote homogeneous dispersion within both single and hybrid metal matrix composites (SMMC and HMMC). The FSP process was carried out using a STANKOIMPORT 6P10 vertical milling machine (Figure 2), known for its high precision and robust construction, which enables the controlled incorporation of nano-reinforcements into the metallic matrix and supports the fabrication of advanced composite structures with improved mechanical performance.

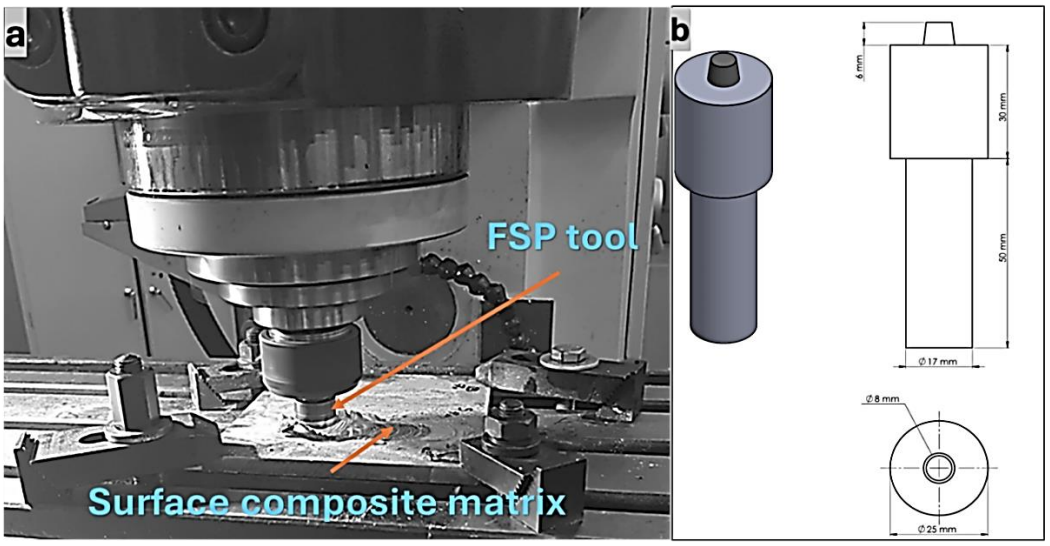

Fig. 1 typical fabrication process using FSP (a) FSP using automatic milling machine, b) FSP tool design.

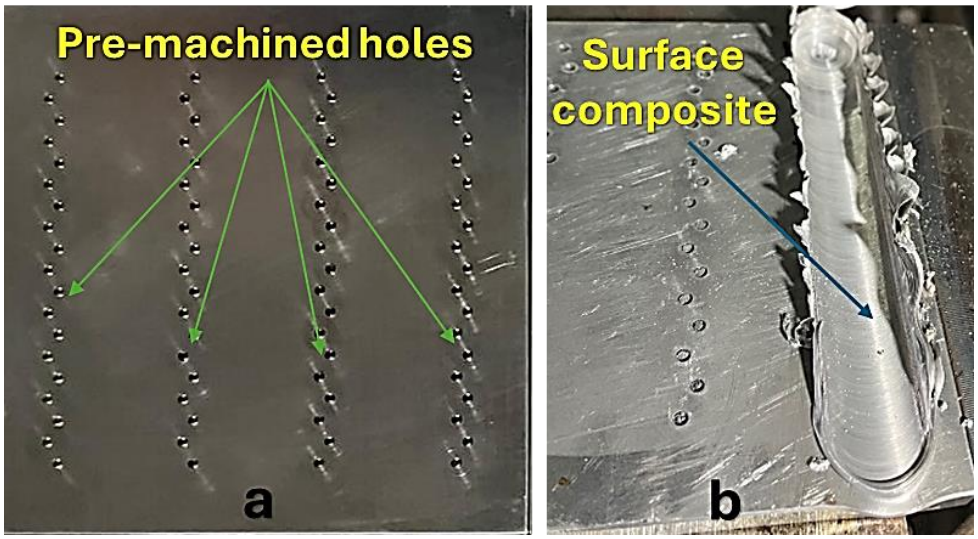

Fig. 2 experimental setup for surface composite fabrication; (a) a metal substrate with an array of pre-machined holes, and (b) the resulting surface composite after processing.

Microstructure Examination

Microstructural characterization involved standard metallographic preparation, including grinding with SiC papers (600–4000 grit), polishing, and chemical etching to reveal the grain structure. The microstructural features of both the base and FSP-processed materials were analyzed using an optical polarized light microscope (UPT203i). This technique facilitated a comparative assessment of microstructural refinement in the as-received AA5083 alloy and in the FSP-treated specimens reinforced with nanoparticles.

Wear Behavior Assessment

The wear performance of the materials was evaluated using a CSM pin-on-disk tribometer (TRB model) at ambient temperature, as shown in Fig.3. The testing procedure followed the ASTM G99-95 standard to ensure consistency and reproducibility. During each test, a constant normal pressure of 0.3 bar was applied while the specimen rotated at a speed of 265 rpm. The pin slid along a circular path with a 3 mm radius on the specimen surface under dry sliding conditions, with no lubrication used. To ensure reliable and comparable results, each test was conducted for a fixed duration of 5 minutes. This standardized approach allowed for consistent evaluation of wear behavior across all samples.

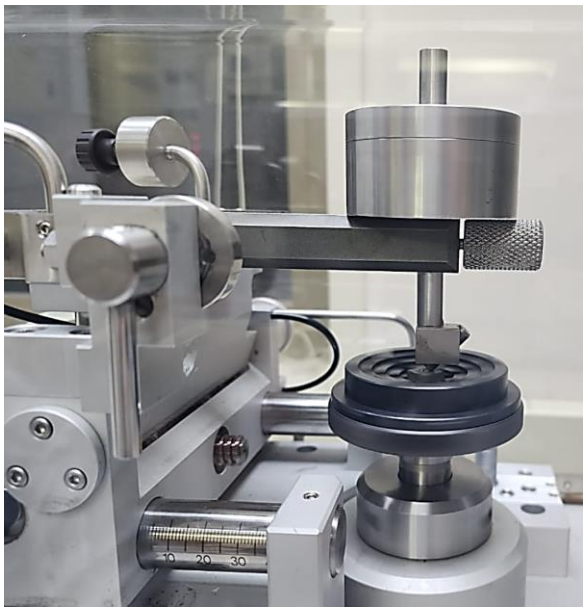

Fig. 3 CSM pin-on-disc tribometer for wear testing.

Corrosion Resistance Evaluation

The corrosion resistance of both the base material and the processed composite specimens was studied using potentiodynamic polarization testing. Electrochemical measurements were performed with a high-precision Autolab PGSTAT 302 N potentiostat/galvanostat system, ensuring accurate control and data acquisition—a 3.5 wt.A 0.9% NaCl solution was used to simulate marine environmental conditions, with tests conducted at room temperature (25 ± 2°C). A conventional three-electrode configuration was employed, where the test specimen served as the working electrode, a platinum foil functioned as the counter electrode, and a saturated calomel electrode (SCE) was utilized as the reference.

RESULTS AND DISCUSSION

Microstructure observation

The grain refinement mechanism in Friction Stir Processing (FSP) is primarily attributed to dynamic recrystallization. During processing, the material undergoes intense plastic deformation and shear, resulting in rapid dislocation accumulation. As frictional heating increases temperature, dislocations become mobile and reorganize into low-energy configurations, forming subgrain boundaries. With continued deformation and thermal input, these evolve into high-angle grain boundaries, nucleating new fine and equiaxed grains. This continuous process within the stir zone, where nucleation and growth co-occur with plastic flow, results in a refined microstructure. The high strain rates and controlled thermal conditions during FSP promote repeated dynamic recrystallization cycles, preventing significant grain growth and enabling the formation of ultrafine or even nanocrystalline structures under optimal conditions. Additionally, the tool's stirring action disrupts coarse intermetallic phases and second-phase particles, which act as grain boundary pinning agents and potential nucleation sites, further enhancing grain refinement. To evaluate FSP's effectiveness quantitatively, average grain size was measured from

microstructural images shown in Fig. 4 (a) and (b), using the Linear Intercept Method (ASTM E112), a standard technique for estimating grain size—particularly suitable for equiaxed structures typically observed after FSP. Figure 4 (a) shows the as-received AA5083 alloy, exhibiting a coarse, elongated grain structure with an average grain size of approximately 285 µm. This is typical of wrought materials shaped by thermomechanical processes like hot rolling. In contrast, Fig. 4 (b) reveals a significantly refined and equiaxed microstructure after FSP, with an average grain size reduced to about 28 µm—a one-order-of-magnitude decrease. This substantial grain refinement is a key outcome of FSP and directly contributes to the improved mechanical properties commonly observed in FSP-treated materials.

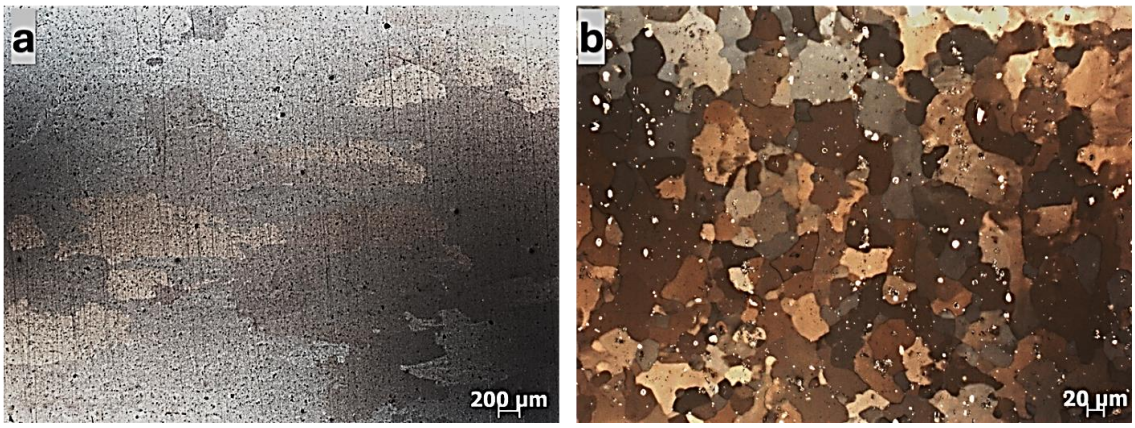

Fig. 4: Microstructure of AA5083 wrought aluminum alloy: (a) base alloy with an average grain size of 285 µm, and (b) after Friction Stir Processing (FSP) showing refined grains with an average size of 28 µm.

Scanning Electron Microscopy (SEM) is crucial for assessing the dispersion of reinforcement particles in metal matrix composites (MMCs), as uniform distribution is essential for improving mechanical properties. Poor dispersion can lead to particle clustering, which creates stress concentration zones and premature failure. Figure 5 presents SEM images that illustrate the dispersion behavior of various single and hybrid reinforcements in an AA5083 aluminum alloy matrix. In single-reinforced composites (Fig. 5, a - c), the dispersion quality depends heavily on the reinforcement type. Figure 5(a) shows AA5083/CNT with a relatively uniform distribution of fine CNTs, despite their tendency to agglomerate due to van der Waals forces. Effective dispersion typically requires advanced processing methods like high-energy ball milling or ultrasonication. In Figure 5 (b), AA5083/G exhibits graphene nanoplatelets (GNPs) that are reasonably well-distributed but show some localized clustering, likely due to their two-dimensional nature and interlayer interactions. Figure 5 (c) illustrates AA5083/BN, where BN particles appear more angular and less uniformly dispersed, with visible clusters. Challenges such as poor wettability during fabrication can hinder their integration into the matrix. Hybrid composites (Figures 5d–f) demonstrate improved dispersion characteristics. Figure 5 (d) (AA5083/CNT+BN) shows finer and more even distribution compared to the single BN composite, suggesting that CNTs may help break up BN clusters, forming a more interconnected network. Similarly, Fig. 5 (e), (AA5083/BN+G) indicates good co-dispersion, with BN

and graphene appearing well integrated, although distinguishing individual graphene layers remains challenging. Finally, Figure 5(f) (AA5083/CNT+G) reveals the most uniform and refined dispersion among all hybrids. The synergistic interaction between CNTs and graphene appears to prevent re-stacking and promote a highly homogeneous microstructure, making this combination particularly effective for composite strengthening.

Microhardness behavior

The incorporation of nano-scale reinforcements led to a significant enhancement in microhardness compared to the base AA5083 alloy. Among the single-reinforced composites, the addition of hexagonal boron nitride (h-BN) resulted in the highest increase, with an average hardness of 78 HV—approximately 27.9% higher than that of the base alloy, as shown in Fig.6. This improvement can be attributed to the high intrinsic hardness of BN particles and their ability to act as practical obstacles to dislocation motion within the metallic matrix. Carbon nanotubes (CNTs) also contributed to a notable rise in hardness (74 HV), representing a 21.3% increase over the base material. The reinforcing effect of CNTs is primarily due to their high aspect ratio and excellent mechanical strength, which facilitates load transfer from the softer matrix to the stiffer reinforcement. However, the effectiveness of CNTs is somewhat limited by challenges related to dispersion and interfacial bonding with the matrix. Graphene-reinforced composites exhibited a moderate improvement in hardness (72 HV), corresponding to an 18.0% increase. While graphene possesses exceptional mechanical properties, its two-dimensional nature makes it prone to agglomeration, which can reduce its reinforcing efficiency. Nevertheless, its presence still contributes positively to the overall strengthening of the composite. The hybrid-reinforced composites demonstrated superior performance compared to their single-reinforced counterparts, highlighting the synergistic effects between different nano-additives. The AA5083/CNT–G composite showed a marked increase in hardness (83 HV), approximately 36.1% higher than the base alloy. The combination of one-dimensional CNTs and two-dimensional graphene likely results in a more interconnected and uniform reinforcing network, effectively impeding dislocation movement and enhancing resistance to plastic deformation. The AA5083/BN–CNT composite displayed an even higher hardness value of 84 HV, indicating a 37.7% improvement over the base alloy. The presence of BN particles may help to prevent CNT agglomeration, while CNTs, in turn, may enhance the dispersion of BN, leading to improved mechanical performance. Notably, the AA5083/BN–G composite achieved the highest hardness value among all tested samples, reaching 86 HV, which corresponds to a 40.9% increase relative to the base alloy. This remarkable enhancement suggests a strong synergistic interaction between BN and graphene, where BN particles may serve as physical barriers to grain boundary movement, while graphene improves load transfer and restricts dislocation glide. Additionally, the refined microstructure resulting from Friction Stir Processing (FSP) likely plays a complementary role in promoting the observed hardness improvements.

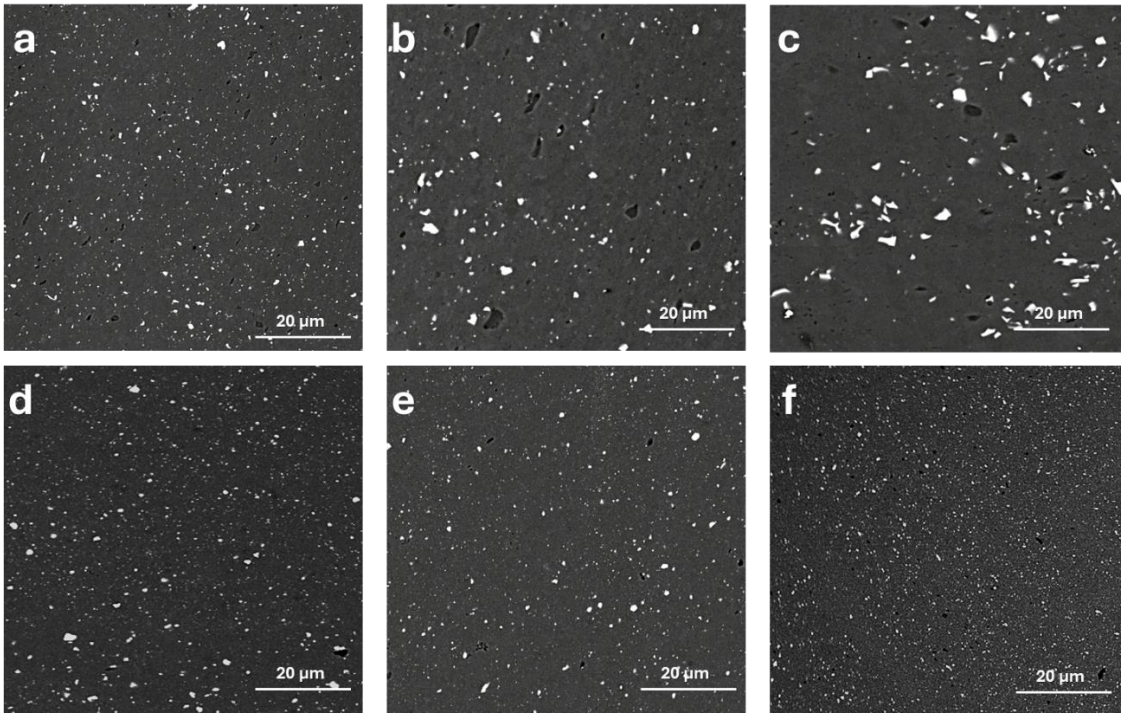

Fig. 5 Scanning Electron Microscopy (SEM) images illustrating the dispersion and distribution of reinforcement particles within the AA5083 aluminum alloy matrix for various single and hybrid composites. (a) AA5083/CNT, (b) AA5083/Graphene, (c) AA5083/BN represent single-reinforced composites. Hybrid composites are shown in (d) AA5083/CNT+BN, (e) AA5083/BN+Graphene, and (f) AA5083/CNT+Graphene.

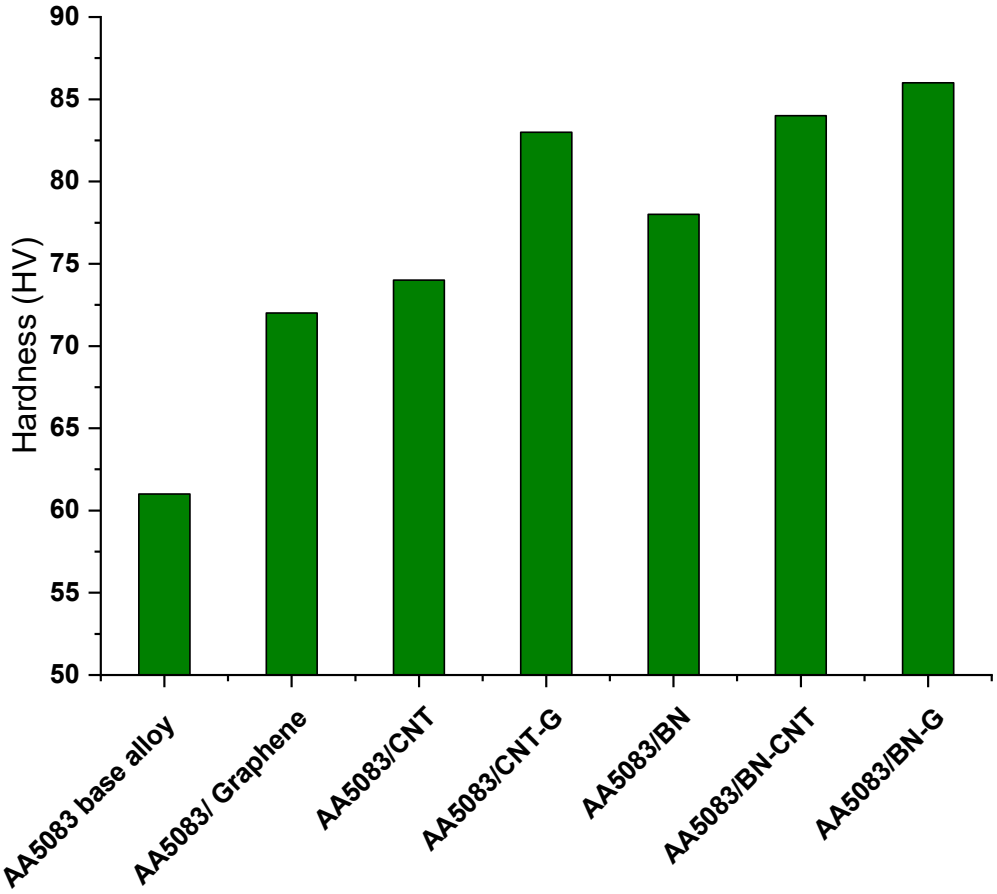

Fig. 6 Comparison of Vickers Hardness (HV) for the AA5083 base alloy and its composites reinforced with single (Graphene, CNT, BN) and hybrid (CNT-G, BN-CNT, BN-G) nanomaterials.

Wear rate analysis

The reduction in wear rate observed in reinforced composites compared to the base AA5083 aluminum alloy highlights the significant role of nano-scale reinforcements in enhancing tribological performance. While individual reinforcements such as graphene, carbon nanotubes (CNTs), and hexagonal boron nitride (h-BN) demonstrated moderate improvements ranging from 14% to 36% reductions in wear rate—hybrid combinations exhibited significantly greater enhancements, suggesting synergistic effects between different reinforcement types , as shown in Fig. 7. Among single-reinforced composites, h-BN showed the most promising results, achieving a 36% improvement in wear resistance due to its high hardness, low friction coefficient, and solid lubrication properties. Graphene contributed to surface protection through its two-dimensional structure but was limited by agglomeration issues, while CNTs acted as effective load-bearing elements, although their one-dimensionality and tendency to cluster somewhat restricted their effectiveness.

Hybrid composites demonstrated superior performance, with AA5083/BN–G exhibiting the lowest wear rate of 0.0232 g/min, representing a 61% reduction

compared to the base alloy. The combination of BN and graphene provided a dual-action mechanism: BN formed a hard, protective layer, while graphene reduced friction and prevented particle re-stacking, resulting in enhanced resistance against both abrasive and adhesive wear. Similarly, AA5083/BN–CNT achieved a 60% reduction in wear rate, where CNTs improved BN dispersion and created uniform reinforcing network. The synergy between different reinforcements also led to multiple wear reduction mechanisms, including hardness enhancement, tribochemical film formation, load transfer, dislocation pinning, and improved dispersion. These findings underscore the importance of hybrid reinforcement strategies in optimizing the mechanical and tribological behavior of aluminum matrix composites for high-performance engineering applications.

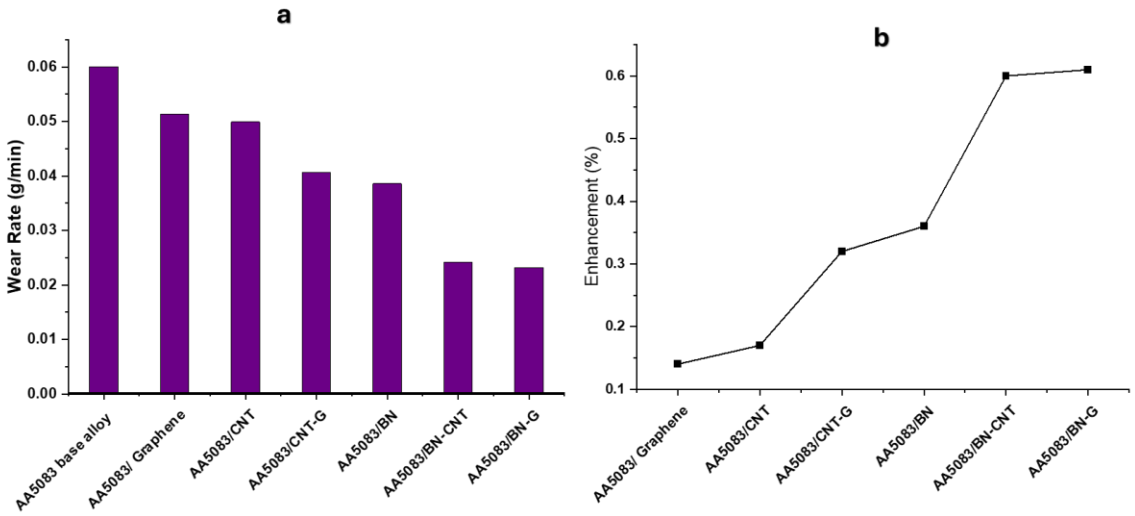

Fig. 7 wear rate analysis (a) wear rate g/min, (b) enhancement behaviour regarding the base alloy.

Corrosion analysis

The electrochemical impedance spectroscopy (EIS) analysis of AA5083-based composites reinforced with various nano-materials (BN), graphene (G), (CNT), and their hybrid combinations, reveals significant insights into their corrosion resistance. The equivalent circuit models fitted to the EIS data incorporate solution resistance (Rs), charge transfer resistance (R), and a constant phase element (CPE) to account for non-ideal capacitive behavior. As shown in table 1, among the tested samples, the CNT-reinforced composite exhibited an exceptionally high charge transfer resistance (110 MΩ), indicating outstanding corrosion resistance. However, its extremely high solution resistance (1.61 MΩ) suggests potential issues with surface contact or electrolyte interaction. Graphene-reinforced composites also demonstrated strong performance, with a charge transfer resistance of 13.8 kΩ, reflecting effective barrier formation and reduced electrochemical activity. In contrast, hybrid-reinforced composites such as BN+CNT and CNT+G showed only moderate improvements in corrosion resistance compared to single reinforcements, suggesting limited synergistic effects under the current processing conditions. The CPE parameters across all

samples indicate varying degrees of surface heterogeneity, with N values below unity confirming non-ideal capacitive behavior due to surface roughness or inhomogeneous coating. Overall, the results highlight the promising role of individual nano-reinforcements, particularly CNTs and graphene, in enhancing the corrosion resistance of AA5083 aluminum alloy, while also pointing to the need for further optimization in hybrid systems to achieve enhanced protective performance.

Table 1 Comparative Analysis and Key Observations

Sample	Rs (Ω)	R (kΩ)	Y_0 (µMho·s^N)	N	Corrosion Resistance
5083+(BN)	31.3	6.3	19.9	0.794	Moderate
5083+(G)	53.3	13.8	18	0.799	High
5083+(CNT)	1.61 MΩ	110 MΩ	230 pMho	0.829	Exceptional
5083+(BN+CNT)	25.6	5.85	12.3	0.886	Moderate
5083+(BN+CNT)	24.6	11.4	13.8	0.824	Moderate
5083+(CNT+G)	35.7	7.04	16.8	0.837	Moderate

Figure 8 presents the corrosion behavior of AA5083-based composites, highlighting both the corrosion rate and the enhancement in corrosion resistance compared to the base alloy. Fig.8 (a) shows that all reinforced samples exhibit lower corrosion rates than the base alloy, indicating improved corrosion resistance. Among the single-reinforced composites, graphene (G) and carbon nanotubes (CNT) demonstrate the most significant reductions in corrosion rate, suggesting their effectiveness as protective reinforcements. Hybrid composites, such as BN+CNT and CNT+G, also show reduced corrosion rates but with varying degrees of improvement. Fig.8(b) quantifies the enhancement in corrosion resistance relative to the base alloy, revealing that hybrid reinforcements like BN+CNT and CNT+G offer substantial improvements (up to 60% and 62%, respectively), while single reinforcements provide moderate enhancements. These results underscore the potential of nano-reinforcements, particularly hybrids, to significantly enhance the corrosion resistance of AA5083 aluminum alloy.

Table 2 show the Comparative Performance of Nano-Reinforced Aluminum Matrix Composites in Terms of Wear Rate, Corrosion Rate, and Hardness . The incorporation of nano-scale reinforcements such as carbon nanotubes (CNTs), hexagonal boron nitride (h-BN), and graphene into aluminum alloys has been widely explored to enhance their mechanical, tribological, and corrosion-resistant properties. The data presented in the table compares the performance of various reinforced composites based on different aluminum matrix alloys, with a particular focus on wear rate (mm^3/m), corrosion rate (mm/y), and hardness (HV). These findings provide valuable insights into how each reinforcement type influences the overall behavior of the composite material. Among the single-reinforced composites, AA5083/graphene exhibits the lowest wear rate of 0.14 mm^3/m and the lowest corrosion rate of 0.0127 mm/y, along with a respectable hardness value of 75 HV. This aligns with previous studies that have highlighted graphene's exceptional mechanical

strength, barrier properties against corrosive elements, and its ability to form low-friction protective layers during sliding. In comparison, AA5083/CNT in the current work shows a slightly higher wear rate than the AA5083/graphene composite but still demonstrates excellent improvements over the base alloy, with a corrosion rate of 0.0119 mm/y and a hardness of 74 HV. CNTs contribute significantly to wear resistance through their high aspect ratio and load-bearing capacity, while also acting as diffusion barriers that slow down corrosion kinetics. However, the one-dimensional nature of CNTs can lead to agglomeration issues, which may limit their full potential unless proper dispersion techniques are employed.

Table 2. Comparative Performance of Nano-Reinforced Aluminum Matrix Composites in Terms of Wear Rate, Corrosion Rate, and Hardness

Reinforcement Type	Composite Type	Wear Rate (mm^3/m)	Corrosion Rate mm/y	Hardness (HV)	Key Observations	Reference
CNT	AA5052/ CNT	0.15	0.02032	80	Excellent improvement in wear and hardness; significant reduction in corrosion current density	[25]
BN	AA5083/BN	0.2	0.02286	74	Good lubrication effect reduces wear; moderate hardness increase	[26]
Graphene	AA5083/ Graphene	0.14	0.0127	75	Superior hardness and corrosion resistance; very low wear rate	[27]
CNT	AA5083/ CNT		0.0119	74		Current work
BN	AA5083/BN		0.0134	78		Current work
Graphene	AA5083/ Graphene		0.0161	72		Current work

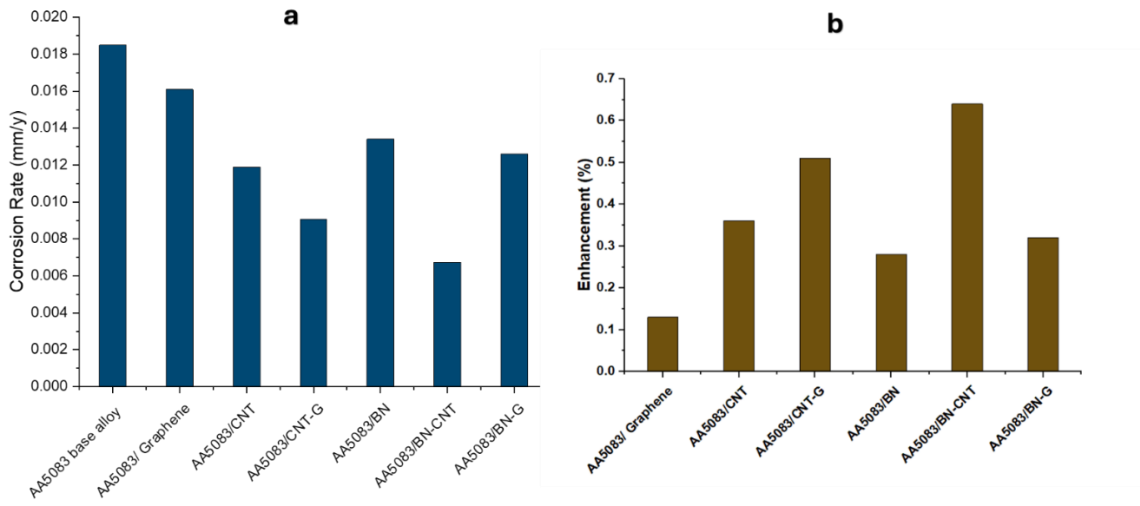

Fig. 8 The corrosion behaviour of the investigated samples, (a) corrosion rate, (b) enhancement of the corrosion rate regarding the base alloy.

AA5083/BN composites display a moderate wear rate of 0.2 mm³/m, a slightly higher corrosion rate of 0.02286 mm/y, and a hardness of 74 HV. The lubricious nature of h-BN contributes to its good wear performance by reducing friction at the contact interface, although its ceramic nature and limited electrical conductivity do not offer the same level of corrosion protection as graphene or CNTs. Nevertheless, BN remains an attractive reinforcement for applications where thermal stability and solid lubrication are critical. When comparing these results to those from other studies, such as AA5052/CNT composites reported, [27], it is evident that the choice of matrix alloy also plays a role in determining the final properties. For instance, AA5052/CNT showed a wear rate of 0.15 mm³/m and a corrosion rate of 0.02032 mm/y, indicating that the AA5083 alloy matrix offers better corrosion resistance when reinforced with CNTs or graphene.

CONCLUSIONS

The incorporation of nano-scale reinforcements into AA5083 aluminum alloy has proven effective in enhancing mechanical strength, wear resistance, and corrosion protection. Graphene, CNTs, and h-BN individually contributed to property improvements, with graphene offering the best balance across all tested parameters. Hybrid reinforcement strategies further amplified these benefits through synergistic interactions, particularly in improving hardness and wear behavior. Corrosion resistance was significantly enhanced with individual nano-additives, especially CNTs and graphene, although hybrid systems require further optimization to maximize protective performance. Overall, the results demonstrate that nano-reinforced aluminum matrix composites are promising candidates for advanced structural and functional applications where durability and performance under harsh conditions are critical.

REFERENCES

1. Das S., Behera R., Datta A., Majumdar G., Oraon B., and Sutradhar G., "Experimental Investigation on the Effect of Reinforcement Particles on the Forgeability and the Mechanical Properties of Aluminum Metal Matr ix Composites", MSA 2010, 01, pp. 310 - 316, (2010). doi:10.4236/msa.2010.15045.

2. Engku A. S., Ku M. N. "Effect of weight percentage of silicon carbide (SiC) reinforcement particles on mechanical behavior of aluminum metal matrix composite", (Al M MC). (2008). http://umpir.ump.edu.my/id/eprint/146

3. Sivananthan S., Ravi K., Samson J. S. C., "Effect of SiC particles reinforcement on mechanical properties of aluminium 6061 alloy processed using stir casting route", Materials Today: Proceedings (2020), 21, pp. 968-970, doi: 10.1016/j.matpr.2019.09.068.

4. Rangrej S., Pandya S., Menghani J., "Effects of reinforcement additions on properties of aluminium matrix composites – A review", Materials Today: Proceedings (2021), 44, pp. 637-641, doi: 10.1016/j.matpr.2020.10.604.

5. Ajagol P., Anjan B.N., Marigoudar R. N., Kumar G. V., "Effect of SiC Reinforcement on Microstructure and Mechanical Properties of Aluminum Metal Matrix Composite", IOP Conf. Ser.: Mater. Sci. Eng. (2018), 376, 012057, doi:10.1088/1757-899x/376/1/012057.

6. Venkatesh, V. S. S., Deoghare, A. B. "Effect of Particulate Type Reinforcements on Mechanical and Tribological Behavior of Aluminium Metal Matrix Composites: A Review" In Lecture Notes in Mechanical Engineering, Springer Singapore, pp. 295-303, (2021).

7. Moustafa, E. B., Melaibari, A., Alsoruji, G., Khalil, A. M., Mosleh, A. O. "Tribological and mechanical characteristics of AA5083 alloy reinforced by hybridising heavy ceramic particles Ta_2C & VC with light GNP and Al_2O_3 nanoparticles", Ceramics Int. (2022), 48, pp. 4710-4721, doi: 10.1016/j.ceramint. 2021.11.007.

8. Jadhav S., Aradhye A., Kulkarni S., Shinde Y., Vaishampayan V., "Effect of hybrid ash reinforcement on microstructure of A356 alloy matrix composite", p.020010, (2019),

9. Samy A. M. and Ali W. Y., "Effect of the thickness and width of artificial turf fiber on the friction and electrostatic charge generated during sliding." Journal of the Egyptian Society of Tribology 16, No. 2, pp. 48-58, (2019).

10. Suresh N., Balamurugan L., Jayabalakrishnan D., "Influence of SiC and WC reinforcements on the mechanical characteristics of AA6061 hybrid metal matrix composites", Proceedings of the Institution of Mechanical Engineers, Part E: Journal of Process Mechanical Eng., 237, pp. 955-970 (2022), doi:10.1177/ 095440892211 41353.

11. Singh R., Kumar A., "A literature survey on effect of various types of reinforcement particles on the mechanical and tribological properties of aluminium alloy matrix hybrid nano composite" Materials Today: Proceedings, 56, pp. 200-208 (2022), , doi: 10.1016/j.matpr.2022.01.068.

12. Son N., Uni N. K., "Influence of Ceramic Particulate Reinforcements on Fly Ash Dispersion Strengthened Composites for Aircraft Structures", (2018).

13. Bandekar N., Prasad M. G. A. "Wear behavior of aluminum hybrid metal matrix composites (HMMCS): a review" (2013), pp. 3.20-23.20.
14. Sharma P., Khanduja D., Sharma S., "Tribological and mechanical behavior of particulate aluminum matrix composites", Journal of Reinforced Plastics and Composites, 33, pp. 2192-2202, (2014), doi:10.1177/0731684414556012.
15. Arunkumar S., Subramani S., Suketh K. M., Vigneshwara S., "A review on aluminium matrix composite with various reinforcement particles and their behaviour" Materials Today: Proceedings 33, pp. 484-490, (2020), doi: 10.1016/j. matpr.2020.05.053.
16. Ali A. S., Youssef M. M., Ali W. Y., and Rashed A., "Triboelectric Nanogenerator Based on Triboelectrification and Magnetic Field", Journal of the Egyptian Society of Tribology 20, No. 2, pp. 1-12, (2023).
17. Taha M., Ibrahim A. M. and Ameer A. K. "Role of hybrid nanofiller GNPs/Al_2O_3 on enhancing the mechanical and tribological performance of HDPE composite." *Scientific Reports* 13, No. 1, p. 12447, (2023).
18. Nabhan A., Nouby M., Hamouda M. M., and Rashed A., "Influence of TiO_2 and SiO_2 nanoparticles additives on the engine oil tribological properties: experimental study at different operating conditions", *International Journal of Advanced Science and Technology* 29, no. 1, pp. 845-855, (2020).
19. Eyad M. A., Ali W. Y., and Nabhan A., "Wear Behavior of Cervical Fusion Plates Fabricated from Polyethylene Reinforced by Kevlar and Carbon Fibers." Journal of the Egyptian Society of Tribology 18, No. 1, pp. 8-17, (2021).
20. Karthikraja M., Ramanathan K., Loganathan K.T., Selvaraj S., "Corrosion behaviour of SiC and Al_2O_3 reinforced Al 7075 hybrid aluminium matrix composites by weight loss and electrochemical methods. Journal of the Indian Chemical Society (2023), 100, 101002, doi: 10.1016/j.jics.2023.101002.
21. Nithyanandhan T., Sivaraman P., Ramamoorthi R., Suresh K., Kannakumar P., Kumar A. N. "Enhancement of corrosion behaviour of AL6061- B4C-RHA reinforced hybri d composite. Materials Today: Proceedings (2020), 33, pp. 372-377, doi: 10.1016/j.matpr.2020.04.167.
22. Aydın F., "A review of recent developments in the corrosion performance of aluminium matrix composites", Journal of Alloys and Compounds (2023), 949, p. 169508, doi: 10.1016/j.jallcom. (2023).169508.
23. Sambathkumar M., Navaneethakrishnan P., Ponappa K., Sasikumar K. S. K., "Mechanical and Corrosion Behavior of Al7075 (Hybrid) Metal Matrix Composites by Two Step Stir Casting Process" Lat. Am. j. solids struct., 14, pp. 243-255, (2017), doi:10.1590/1679-78253132.
24. Kssucitharan J. R. D., "An Overview on Development of Aluminium Metal Matrix Composites with Hybrid Reinforcement", IJSR, 1, pp. 196-203, (2012), doi:10.21275/ijsr13010104.
25. Samal P., Vundavilli P. R., Meher A., Mahapatra M. M., "Reinforcing effect of multi-walled carbon nanotubes on microstructure and mechanical behavior of AA5052 composites assisted by in-situ TiC particles", Ceramics International (2022), 48, pp. 8245-8257, doi: https://doi.org/10.1016/j.ceramint.2021.12.029.

26. Ammar H. R., Sherif E. M., Sivasankaran S., Almufadi F. A., Mekky A. H., "Developing Improved Corrosion-Resistant AA5083—BN/WC Composites for Tribological Applications", Materials (2023), 16, doi:10.3390/ma16041663.
27. Sadabadi H., Ghaderi O., Kordijazi A., Rohatgi P. K., "Graphene derivatives reinforced metal matrix nanocomposite coatings: A review", Journal of Metals, Materials and Minerals (2022), 32, pp. 1-14, doi:10.55713/jmmm. v32i3.1518.